Full Length Research Paper

Entrainment mass transfer in annular flow regime of two-phase carbon dioxide

Zahra Baniamerian[1]*, Ramin Mehdippour[1] and Cyrus Aghanajafi[2]

[1]Department of Mechanical Engineering, Tafresh University of Technology, Tafresh, Iran.
[2]Department of Mechanical Engineering, Khaje Nasir Toosi University of Technology, Tehran, Iran.

Having more heat transfer rate and lower pressure drop, along with better environmental treatment, carbon dioxide has drawn the attention of many researchers. Most of the two-phase heat transfer analyses are involved in estimation of dry-out phenomenon in order to avoid heat transfer drops. Entrainment, because of having great influence on dry-out occurrence, is studied in this article. Most of the available models for entrainment are experiment-based and therefore applicable in restricted conditions. In the present study, a physical model is proposed for simulation of entrainment in annular flow regime of liquid-vapor in a vertical tube. The tube is supposed to be warming up by a constant and uniform heat flux applied on its lateral area. The proposed model is general and can be applied to all kind of fluids of different working conditions; it is verified with some experimental data available in the literature. Entrainment contribution of mass transfer is compared with evaporation contribution through introducing a factor which is called "Mass Transfer Ratio" (MTR). The magnitude of this factor demonstrates the significance of entrainment phenomenon. MTR factor is compared with some widely-used working fluids.

Key words: Carbon dioxide, working fluid, entrainment, dry out, mass transfer.

INTRODUCTION

Non-toxicity, non-flammability, easy availability, low price, no need of recycling, and compactness of components are the characteristics that has signified carbon dioxide among other refrigerants. Many experiments have been accomplished to compare heat transfer and pressure drop of two-phase carbon dioxide with some other refrigerants (Zhao and Bansal, 2007; Choi et al., 2007; Thome and Ribatski, 2005; Choi et al., 2007; Oh et al., 2008; Yun et al., 2005). All the available relevant researches in the literature emphasizes that heat transfer coefficient of carbon dioxide is much more than common refrigerants. Choi et al. (2007) have found in their experiments that the mean heat transfer coefficient ratio of R-22: R-134a: CO_2 is approximately 1.0:0.8:2.0. They claimed that the heat transfer coefficient of CO_2 is higher than that of R-22 and R-134a during evaporation under

all test conditions. The higher heat transfer coefficient of CO_2 is believed to be due to its high boiling nucleation that is associated with its different thermo-physical properties. Table 1 provides a comparison between physical characteristics of carbon dioxide, R11, R12, R22, and R134a at saturation conditions at $T = 0°C$.

Due to the low critical temperature ($T_{crit.} = 31.1°C$) and high critical pressure ($p_{crit.} = 73.8 bar$) carbon dioxide is utilized at much higher operating pressures as compared to other conventional refrigerants. The higher operating pressures result in high vapor densities, very low surface tensions, high vapor viscosities and low liquid viscosities and thus yield flow-boiling heat transfer and two-phase flow characteristics that are quite different from those of conventional refrigerants (Cheng et al., 2006). Considering the mentioned differences, the available empirical models of heat and mass transfer that are mostly obtained based on applying other refrigerants are not in cooling systems with CO_2 as working fluid.

---
*Corresponding author. E-mail: rr_amerian@yahoo.com, amerian@tafreshu.ac.ir. Tel: +98 8626227125.

Table 1. Physical properties of CO_2, $R134a$, $R22$, $R12$ and $R11$ at $T = 0°C$ and saturation conditions.

Refrigerant	$p(MPa)$	$\rho_f(kg/m^3)$	$\rho_g(kg/m^3)$	$\mu_f(\mu Pa.s)$	$\mu_g(\mu Pa.s)$	$\sigma(N/m)$	ρ_f/ρ_g	μ_f/μ_g
CO_2	3.5	926.47	98.14	99.112	14.803	0.00451	9.44	6.695
$R134a$	0.29	1294.5	14.45	266	10.72	0.01154	89.58	24.81
$R22$	0.5	1281.1	21.312	215.7	11.369	0.01167	60.11	18.97
$R12$	0.3082	1396.1	17.873	245.22	10.611	0.011772	78.11	23.11
$R11$	0.0402	1534.1	2.4797	523.19	9.329	0.02098	618.66	56.08
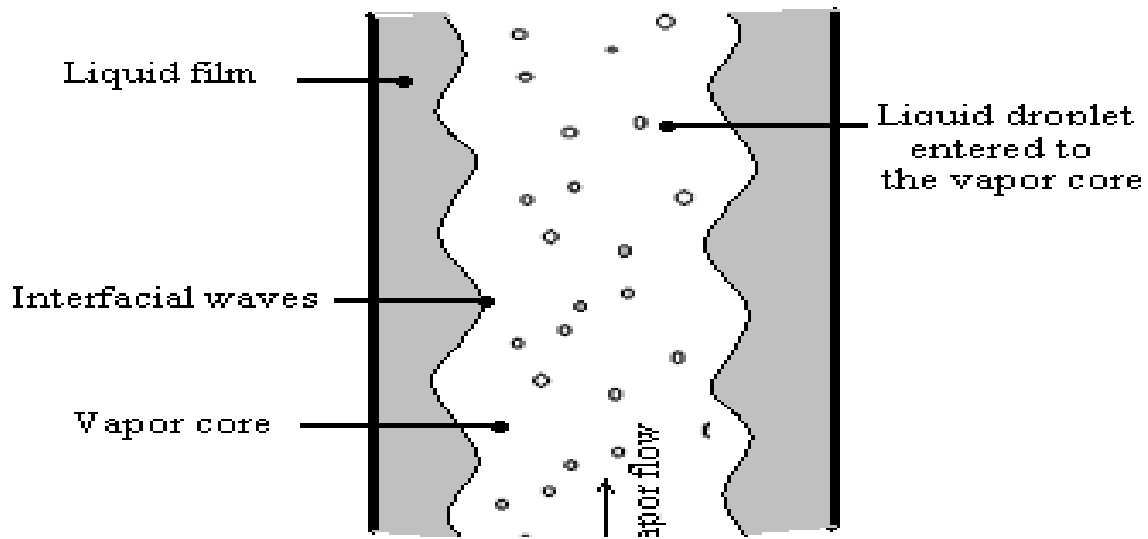
Figure 1. Schematic of interfacial waves and ripples in a typical annular two-phase flow.

In this regard, studying entrainment phenomenon in CO_2 should be started from the fundamental physics of the problem. This is what has been accomplished in the present article. As vapor flows upon a liquid phase in the annular flow regime, some waves on their interface form and begin to grow (Figure 1). These waves, called interfacial waves, strongly influence the fluid flow. In annular flow regime, entrainment mass transfer occurs due to the effects of interfacial waves formed between liquid film and vapor core. In other word, as the interfacial stress exceeds the retentive force of surface tension, liquid droplets start to transfer into the vapor core in the annular flow regime. Entrainment mass transfer is known to occur through three mechanisms:

1. Undercutting waves crest by the flowing vapor
2. Bursting of bubbles at the interface
3. Impingement of existing droplets of vapor core to the surface of liquid film.

Among these, the first mechanism provides the major portion of entrainment and is of more interest. First mechanism is associated with deformation of interfacial wave crests by the flowing vapor. This deformation continues by sliming the wave crest from a point until it will be ruptured. The ruptured part of the wave crests may accelerate into vapor core and forms the entrained droplets in the core.

Entrainment mass transfer as an important issue affecting heat transfer and fluid flow behavior has been studied for many years. Most of the accomplished researches in this field are experimental and have been carried out at restricted operating conditions and on some special fluids like water and some limited number of refrigerants (Pan and Hanratty, 2002; Barbosa et al., 2002; Kataoka et al., 2000; Sawant et al., 2008).

Most of the available correlations for entrainment are empirical and based on experiments that have employed water or R-series refrigerants as working fluid. These correlations due to major differences between the thermo-physical behavior of carbon dioxide and common refrigerants seem not useful to be applied for carbon

dioxide. The main objective of this study is to obtain a general correlation for computation of entrainment and to measure the significance of entrainment mass transfer contribution in compare with other refrigerants. The significance of the entrainment phenomenon is studied through comparing its contribution with the rate of evaporation as the most sensible mass transfer in two-phase flows.

PHYSICAL CONCEPT OF ENTRAINMENT PHENOMENON

Flowing high speed vapor phase over the liquid phase in the annular flow regime commonly results in formation of some waves at their interface (Figure 1). These waves play an important role in occurrence of entrainment mass transfer. Since liquid droplets transfer into vapor core as a result of the mechanism of undercutting the waves crests. Although, some other mechanisms have been introduced to be the potential of the entrainment (Hewitt and Hall-Taylor, 1970), the undercutting mechanism is merely focused in the present study.

There are many studies in the literature concerned with formation of waves but most of these are not engaged with its consequent influences. As claimed by Thome and Collier (1996), interfacial waves of different fluids form in different fluid velocities that are directly dependent on thermo-physical properties of each fluid.

Using high-speed cinematography, Woodmansee and Hanratty (1969) observed that the principal means of droplet entrainment from a liquid film into vapor core are the rapid acceleration, lifting, and subsequent shattering of ripples on the liquid-vapor interface.

There are many entrainment models, available in the literature, which are most empirical and more based on dimensionless groups rather than physical potentials of entrainment. In the present study, it is assumed that the entrainment takes place as a result of sweeping a fraction of wave crest off into the vapor core (Baniamerian and Aghanajafi, 2010). Regarding this assumption, entrainment rate depends on the volume of liquid cut off from the wave crest, wave length, number of waves and the wave propagation velocity. The aforesaid statement can be simply formulated as (Baniamerian and Aghanajafi, 2010):

$$E = \frac{\forall_l \cdot \rho_l \cdot}{t_w \cdot A_{co}} (\frac{P_{co}}{\lambda} \times \frac{L}{\lambda})$$ (1)

In the relation earlier mentioned, $((P_{co}/\lambda) \times (L/\lambda))$ accounts for number of waves in the control volume. Interfacial area through which liquid droplets transfer into the vapor core is:

$$A_{co} = P_{co} \times L$$ (2)

And the period of entrainment phenomenon is written as:

$$t_w = \frac{\lambda}{u_g - u_l}$$ (3)

Where, u accounts for flow velocity and indices l and g denote liquid and vapor phase respectively. It can be found that determination of interfacial waves characteristics, including wave amplitude, length, velocity and frequency, are the first steps of mass transfer calculations.

Simulation of interfacial waves

When a light fluid flows over a layer of a heavier one, their interface becomes unstable when the relative velocity exceeds a critical speed. This instability, known as Kelvin-Helmholtz instability, may occur at the interface of miscible or immiscible fluids, or within a single fluid in the region of a strong density gradient (Hewitt and Hall-Taylor, 1970). The Kelvin-Helmholtz instability is of great importance in annular flow heat and mass transfer behavior. For an unstable annular flow, interfacial waves grow/decay exponentially in their amplitude as time spends. While on the contrary, experimental observations found interfacial waves of relatively steady amplitudes in typical annular flows. This issue demonstrates that the interfacial waves of common annular flow regimes are of stable condition and can be assumed to have constant amplitude and wave length. Interfacial waves are assumed to be sinusoidal.

By exerting the condition for neutrally stable waves based on Kelvin-Helmholtz theory, the wave length can be written as (Baniamerian and Aghanajafi, 2010):

$$\lambda = \frac{2\pi}{(u_g - u_l)^2 (\rho_g/\sigma) - (2\rho_g/\rho_l \delta)}$$ (4)

The wave amplitude can be computed from the following correlation (Baniamerian and Aghanajafi, 2010):

$$\varepsilon/(D_h - 2\delta) = 121\sqrt{2}/(\text{Re}_g \sqrt{C_f})$$ (5)

Where, C_f, Re_g, D_h account for the liquid frictional factor, vapor Reynolds Number and the pipe hydraulic diameter respectively. (Calculation of the wavelength and amplitude are comprehensively mentioned at the previous work of authors (Baniamerian and Aghanajafi, 2010)).

After performing these computations, at this stage to calculate the volume of transferred liquid into vapor core, the disjoining point of the wave should be determined. This point is obtainable through a force analysis on the waves.
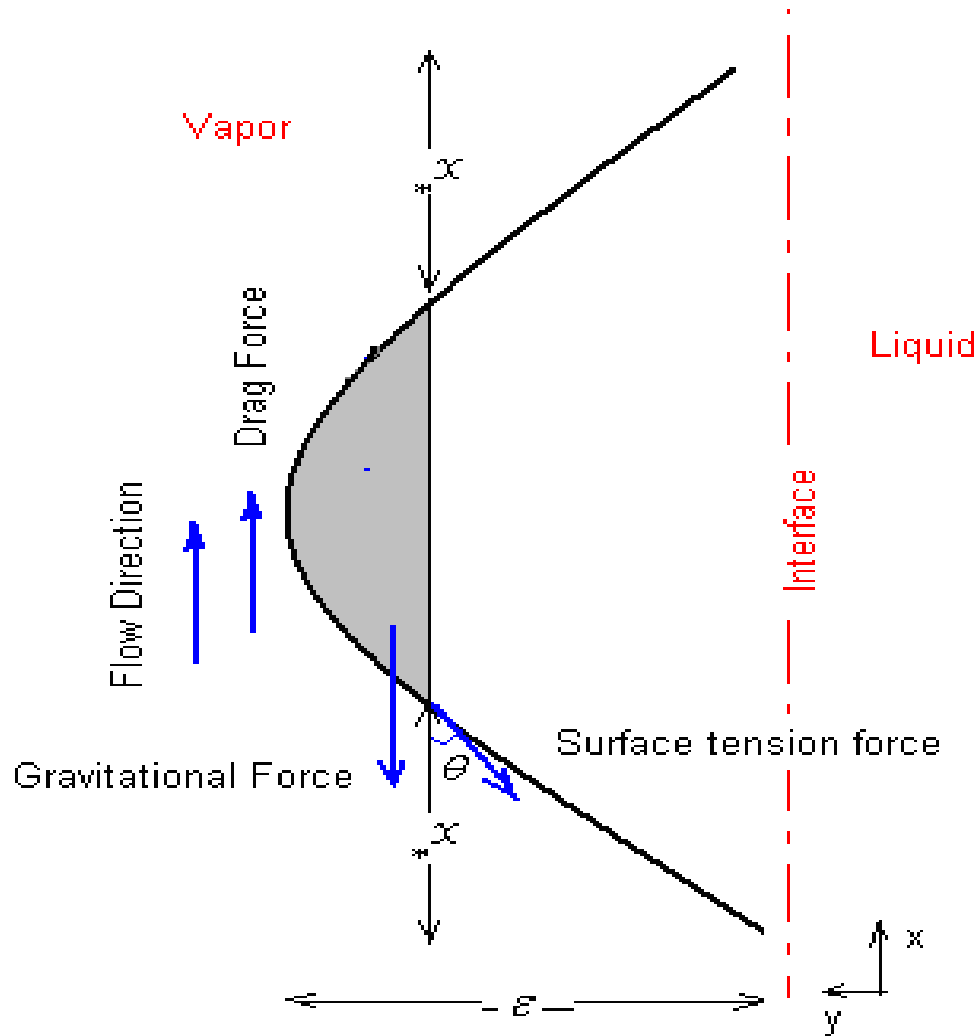
Figure 2. Forces act on a typical interfacial wave.

Force balance on interfacial waves

The force balance on the wave is applied to find the disjoining point of wave. Forces which act on a typical wave are shown in Figure 2. As demonstrated in the mentioned figure, surface tension force is assumed to exert just on the wave front because the wave usually flattens in the rear to experience the least possible surface tension force (Holowah and Hochreiter, 2002). As demonstrated in Figure 2, the exerted forces on the crest include interfacial drag, surface tension force and gravity. At this stage, the mentioned forces are calculated individually.

Interfacial drag

The first considered force is the interfacial drag and is of following form:

$$\tau_i = \frac{1}{2} f_i \rho_{co} A_{co} u_{co}^2 \tag{6}$$

ρ_{co} and u_{co} are the homogeneous density and velocity of vapor core.

Interfacial shear stress computation is performed in the work of Holowach and Hochreiter (2002) by applying liquid density and velocity instead of those of vapor core. In the present study, applying interfacial shear stress in form of Equation 7 results in better consistency with experimental results of similar conditions. Therefore, vapor core characteristics are applied to obtain interfacial shear stress. Interfacial friction factor f_i can be obtained applying Whalley-Hewitt correlation (Collier and Thome, 1996):
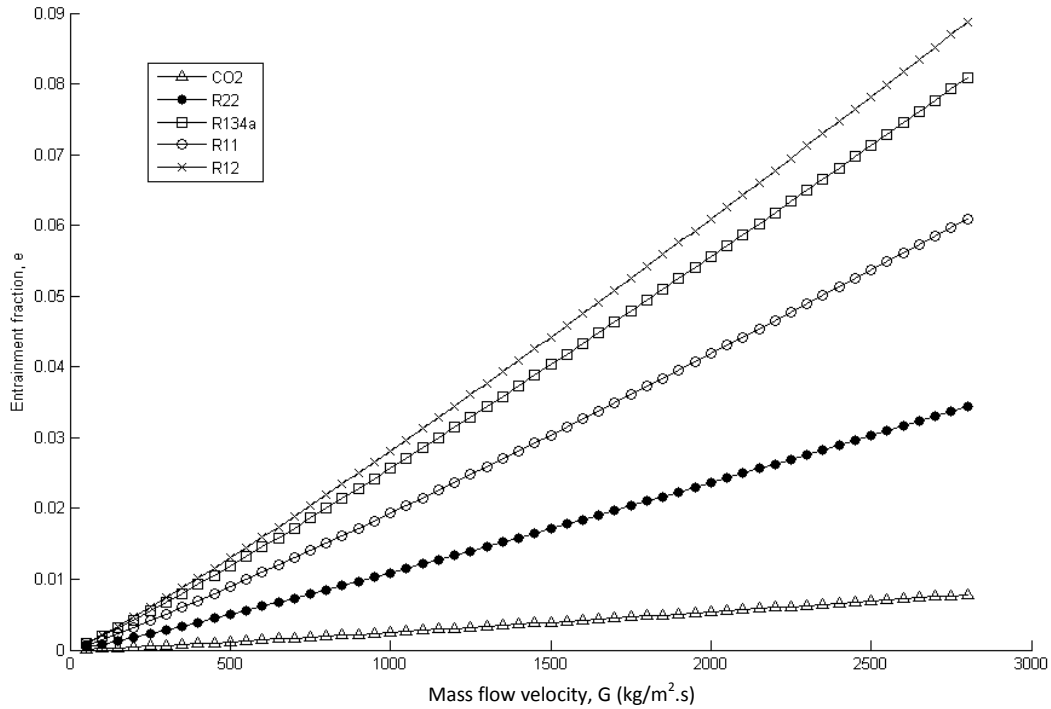
Figure 3. Variation of entrainment fraction against mass flow velocity; comparison between CO2, R11, R12, R22, and R134a.

$$\frac{f_i}{f_g} = 1 + 24\left(\frac{\rho_l}{\rho_{co}}\right)^{1/3}\frac{\delta}{D} \tag{7}$$

Where f_g, is the vapor core frictional factor that can be obtained by applying Muddy diagram (Currie, 1981).

The area on which drag force acts can be calculated as follows:

$$A_{disjoining} = \int_{x^*}^{\lambda/2-x^*}\varepsilon\sin(kx)dx - \left[\varepsilon - \varepsilon\sin\left(kx^*\right)\right]\left(\frac{\lambda}{2} - 2x^*\right) \tag{8}$$

Where, x^* demonstrates axial position of wave disjoining point (Figure 3).

Gravitational force

The volume of the liquid disjoined from the wave should be calculated to obtain gravitational force. This volume can be computed by applying disc integration over the limits demonstrated in Figure 3. The volume is written in terms of axial coordinate of disjoining point (Holowach and Hochreiter, 2002):

$$k^* = 2\pi x^*/\lambda$$

$$\forall_l = \frac{\varepsilon\lambda^2}{4\pi}\left[-2 + 2\sin k^* + 2\left(1-\sin^2 k^*\right)^{1/2}\cos^{-1}\left(\sin k^*\right) - \sin k^*\left(\cos^{-1}\left(\sin k^*\right)\right)^2\right] \tag{9}$$

Then the gravitational force can be achieved:

$$F_g = \rho_l\forall_l g \tag{10}$$

Surface tension force

The surface tension force on the front of the wave is calculated through following correlation:

$$F_\sigma = \sigma K A_\sigma \tag{11}$$

Where, σ, $K_{crest,avg}$, A_σ, account for surface tension, average curvature of the wave crest, and the effective area on which the surface tension force acts, respectively.

The curvature of the wave of sinusoidal form can be calculated using the following relation (Thomas, 2002):

$$K = \left|-\left(k^2\varepsilon\right)\sin(kx)\right|\Big/\left[1 + \left((k)\cos(kx)\right)^2\right]^{3/2} \tag{12}$$

It is assumed for simplicity that the area on which the surface tension force acts is a semi-circle of

diameter $\left(\lambda/2 - 2x^*\right)$. This assumption is based on the wave deformation (Holowach and Hochreiter, 2002):

$$A_\sigma = \frac{\pi}{8}\left(\lambda/2 - 2x^*\right)^2 \tag{13}$$

The surface tension force acts tangential to the wave profile and since in this study the sinusoidal profile is assumed for the wave, the angle, θ shown in Figure 3 is:

$$\theta = \tan^{-1}\left(k\varepsilon\cos(kx)\right) \tag{14}$$

Substituting relations (12 to 14) into Equation 11 results in:

$$F_\sigma = (\pi/8)\sigma\left\{\left|-k^2\varepsilon\sin(kx^*)\right|\Big/\left[1 + \left(k\cos(kx^*)\right)^2\right]^{3/2}\right\}\left(\lambda/2 - 2x^*\right)^2 \tag{15}$$

As mentioned earlier, the forces which act on wave profile are surface tension, drag and gravity. The point at which these forces balance is assumed the disjoining point of wave, since after this point the drag force prevails the retentive force of surface tension and result in sweeping a little part of wave off and transferring into the vapor core. The exact coordinate of the disjoining point can be achieved through applying a force balance on the wave:

$$F_D + F_\sigma - F_g = 0 \tag{16}$$

Substituting the value of each force in the above relation results in an implicit equation with a single unknown of x^* that can be solved by try and error method.

At this stage, all the variables in Equation 1 have been calculated. It should be noted that the computed value result from Equation 1 is the maximum value of the entrainment and it is not necessarily equal to the real entrainment rate which can be measured through experiments. This issue is the result of returning a little fraction of the swept-off wave into the liquid film again because of prompt acceleration of flow in the vapor core. On the other hand, some empirical correlations have been employed during calculation of friction factor and wave amplitude that may exert some errors in our model. Therefore, Equation 1 should be modified by utilizing a correction factor. In order to obtain an appropriate correction factor, we have applied the experiment results of Utsuno et al. (1998) cited in Steinke and Kandlikar (2004). The correction factor is of following form:

$$CF = 2.5\left(\frac{\rho_g}{\rho_l}\right)^4\left(\frac{1}{\sigma}\right) \tag{17}$$

Note that the factor 2.5 is not dimensionless. Therefore, the final form of the entrainment rate correlation will be:

$$E = 2.5\left(\frac{\rho_g}{\rho_l}\right)^4 \frac{\forall_l.\rho_l.\left(u_g - u_l\right)}{\lambda^3\sigma} \tag{18}$$

Entrainment rate has made dimensionless through dividing by total mass flow rate and named "entrainment fraction" e.

$$e = \frac{E}{G} \tag{19}$$

The tube is assumed to be warming up by constant and uniform heat flux similar to the condition applied in experiment of Utsuno et al. (1998) cited in Steinke and Kandlikar (2004). Experiment of Utsuno et al. (1998) cited in Steinke and Kandlikar (2004) has been accomplished in the pressure range of $3 < p < 9 Mpa$ and Reynolds number range of $5.4\times10^3 < \mathrm{Re} < 3.5\times10^5$. The exerted heat flux in their set of experiments is varied from 0.33 to $2\ MW/m^2$.

The most sensible contribution of mass transfer in two-phase flows is evaporation. Therefore, evaporation can be a good criterion for evaluation of other mass transfer contributions. Evaporation rate is estimated through the following relation:

$$\dot{m}_{evap} = \frac{q^{//}}{h_{fg}} \tag{20}$$

As mentioned earlier in the present study, the significance of entrainment mass transfer contribution is evaluated. It is worth introducing a dimensionless factor, named mass transfer ratio, which represents the ratio of entrainment mass transfer to the evaporation contribution:

$$mass\ transfer\ ratio = \frac{m_{en}}{m_{ev}} \tag{21}$$

RESULTS AND DISCUSSION

A computer program is developed to calculate the exact fraction of liquid that is cut off by the shearing force of high-speed flowing vapor at the pipe core. The proposed correlation for entrainment is compared with some empirical correlations and deviations are tabulated in Table 2. Since most of available empirical correlations are obtained from experiments on water as working fluid, therefore thermo physical characteristics of water are employed in Equation 18 to achieve an acceptable

Table 2. Comparison between empirical correlations of entrainment rate and the suggested correlation.

Reference	Working fluid	Correlation of entrainment	Mean deviation[*] (%)	Average deviation[**] (%)
Ishii-Mishima (Sawant et al., 2008)	Water-air	$G_e = G(1-x)\tanh\left(7.25\times10^{-7}\,\mathrm{Re}_l^{0.25}\,We_g^{1.25}\right)$ $We_g = \rho_g j_g^2 d / \sigma \left(\Delta\rho/\rho_g\right)^{1/3}$	1.5	1.5
Hewitt (Hewitt and Whaley, 1978)	Water-air	$\mathrm{Re}_\infty = \exp\left(5.8504 + 0.4249(\mu_g/\mu_l)\sqrt{\rho_l/\rho_g}\right)$ if $\mathrm{Re}_l < \mathrm{Re}_\infty$ $G_e = 0$ if $\mathrm{Re}_l > \mathrm{Re}_\infty$ $G_e = 5.75\times10^{-5}\alpha_g\rho_g u_g\left[(\mathrm{Re}_l - \mathrm{Re}_\infty)^2\left(\mu_l^2/d\sigma\right)\rho_l/\rho_g^2\right]^{0.316}$	0.5%	-0.1
Sawant et al., 2008	Water-air	$\mathrm{Re}_{film} = 250\log\mathrm{Re}_l - 1265,\ \ We_g = \rho_g j_g^2 d / \sigma\left((\rho_l - \rho_g)/\rho_g\right)^{0.25}$ $G_e = G(1-x)(1 - \mathrm{Re}_{film}/\mathrm{Re}_l)\tanh\left(2.31\times10^{-4}\times\mathrm{Re}_l^{-0.35}\,We_g^{1.25}\right)$	15%	15
Schadel et al., 1990	Water-air	$\mathrm{Re}_\infty = \exp\left(5.8504 + 0.4249(\mu_g/\mu_l)\sqrt{\rho_l/\rho_g}\right)$ if $\mathrm{Re}_l < \mathrm{Re}_\infty, G_e = 0$ if $\mathrm{Re}_l > \mathrm{Re}_\infty$ $G_e = 1.175\times10^{-4}u_g\mu_l(\mathrm{Re}_l - \mathrm{Re}_\infty)\sqrt{\rho_l/\rho_g}$	5.5%	-4.3
Okawa et al., 2003	Water-steam	$f_i = 0.005(1 + 300\,\delta/d)$ $Ge = 4.79\times10^{-4}\left(\rho_l/\rho_g\right)^{0.111}\rho_l\rho_g f_i\, j_g^2 \delta/\sigma$	2.1%	2.1
Ueda (Kataoka et al., 2000)	Alcohol-air	$U = (\tau_i/\sigma_l)(\alpha_l v_l/\sigma_l)^{0.6}$ $G_e = 3.54\times10^{-3}U^{0.57}$	4.8%	4.8
Utsuno-Kaminaga (Steinke and Kandlikar, 2004)	Water-Steam	$G_e = G(1-x)\tanh\left(0.16\,\mathrm{Re}_l^{0.16}\,We_g^{0.08} - 1.2\right)$ $We_g = \rho_g j_g^2 d / \sigma\left(\Delta\rho/\rho_g\right)^{1/3}$	0.84%	-1.28

$$* \ \mathrm{Mean\ deviation} = \frac{1}{N}\sum_{i=1}^{N}\frac{\left||m_{en}|_{\text{present model}} - |m_{en}|_{\text{experiment}}\right|}{m_e|_{\text{experiment}}}\times100\%$$

$$** \mathrm{Average\ deviation} = \frac{1}{N}\sum_{i=1}^{N}\frac{|m_{en}|_{\text{present model}} - |m_{en}|_{\text{experiment}}}{m_e|_{\text{experiment}}}\times100\%$$

comparison between the present and other available models.

Variation of entrainment fraction via mass flow velocity for the four widely-used refrigerants and carbon dioxide is plotted and depicted in Figure 3. It is found that increment in mass flow velocity increases the amount of entrainment. In order to justify this phenomenon, mass velocity influences on the interface wave amplitude and wavelength are evaluated and displayed in Figure 4. Increasing in mass velocity decreases wave amplitude and wavelength. The first leads to a decrease in entrainment rate while the second increases the entrainment contribution through increasing total number of waves. Results of computer program demonstrate that the second issue is more effective than the first one (Figure 4).

As shown in Figure 3, entrainment contribution of mass transfer in carbon dioxide is much less than that of R11, R12, R22 and R134a. This issue is due to specific thermo-physical characteristics of carbon dioxide that make it different from other refrigerants (Table 1).

Variation of entrainment fraction via surface tension

changes is plotted and shown in (Figure 5). It is found that the amount of entrainment decreases with increasing the fluid surface tension. Increasing in the fluid surface tension, increases the amplitudes of waves propagating at the interface which in turn increases the entrainment rate potentially. On the other hand, wavelength increases with surface tension which results in a decrement in number of interfacial waves. When interfacial waves increase in amplitude, they will be more vulnerable of being cut off by vapor core and a larger amount of liquid enters through the vapor core. Results display that decrease in number of waves prevails the increase in wave's amplitude and at last decreases the entrainment rate with the fluid surface tension.

The other parameter which has been considered in this study is the effect of pipe diameter. In pipes of larger diameter, entrainment fraction is more than those of smaller ones. Variation of entrainment rate in different pipe diameters is depicted in Figure 6. It deems that after some diameters, further increment in pipe diameter does not considerably affect entrainment mass transfer.

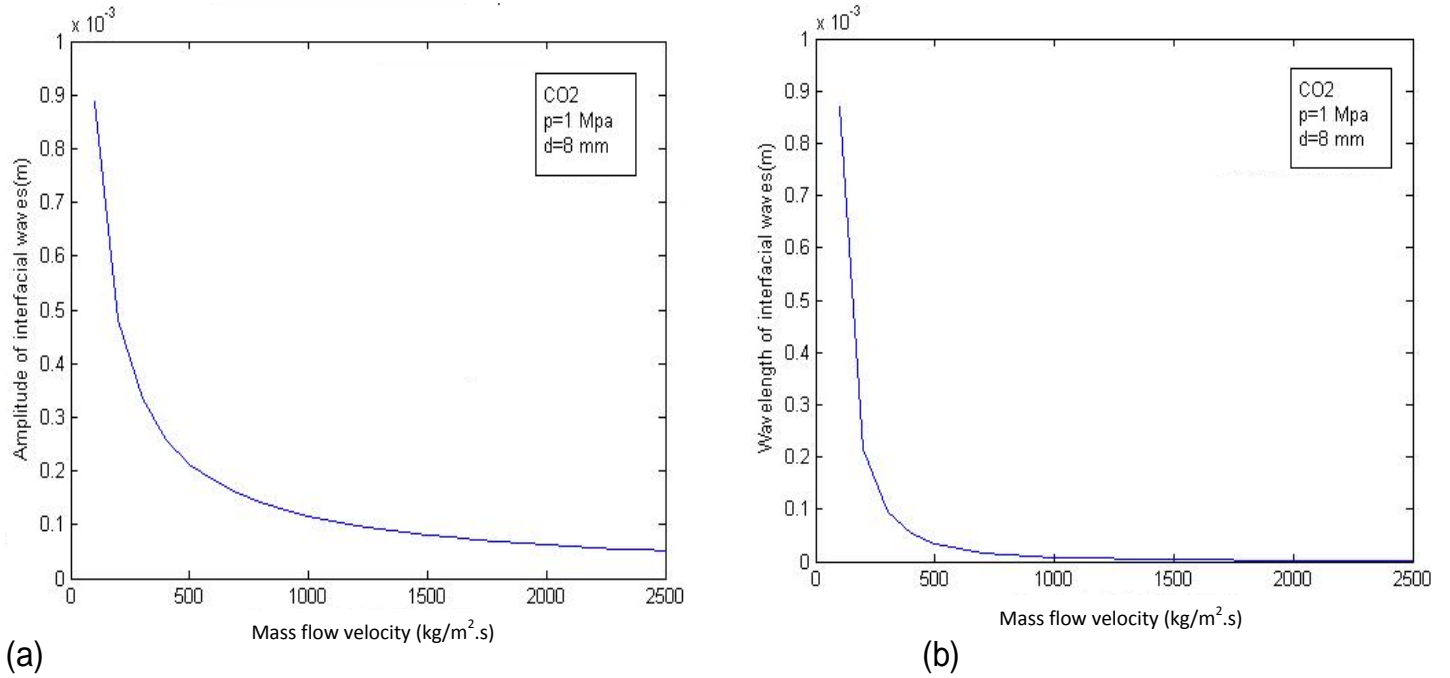Variation of mass transfer ratio against wall heat flux is

Figure 4. Effects of mass flow velocity on (a) Amplitudes (b) wavelength of interfacial waves.
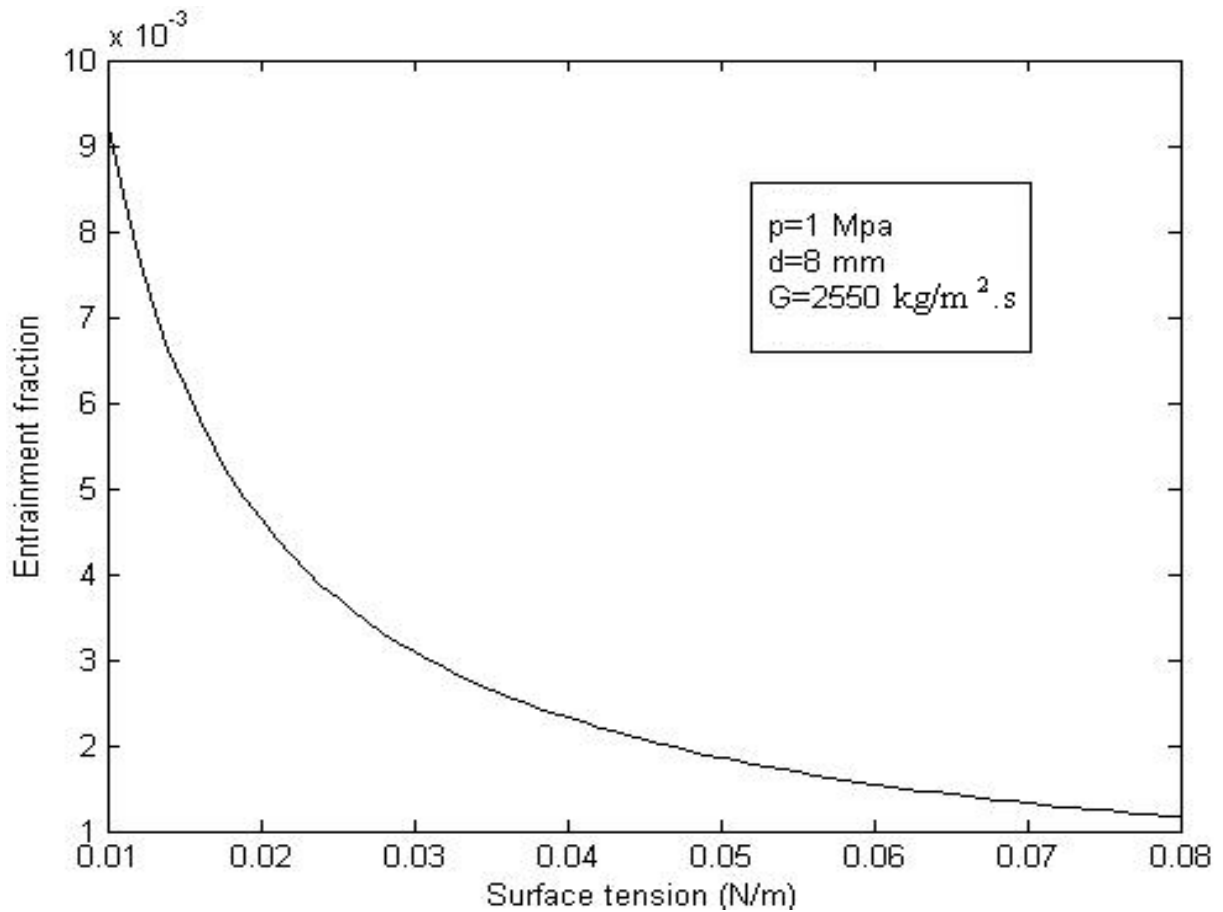

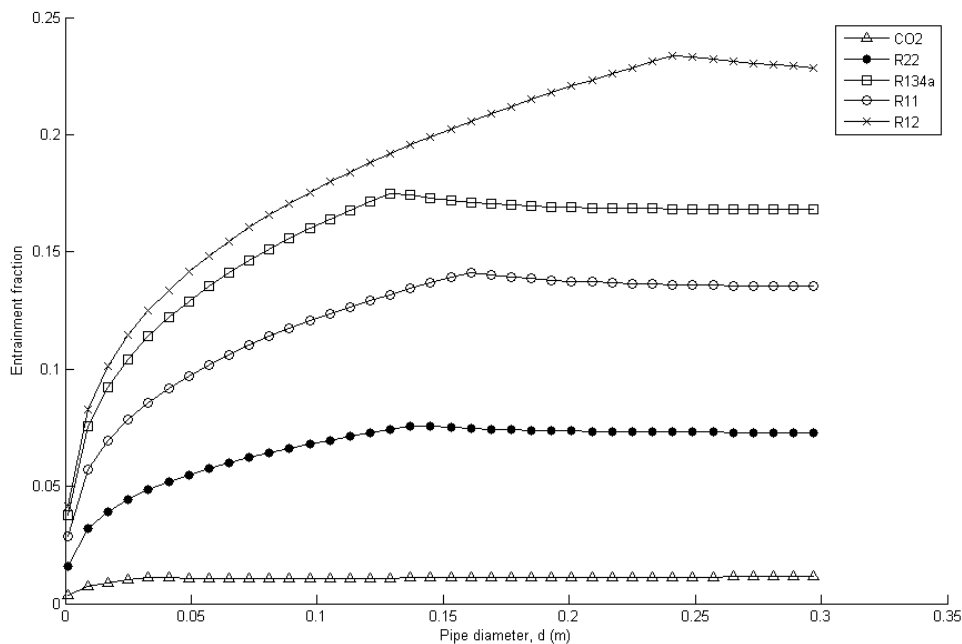**Figure 5.** Variation of entrainment fraction against surface tension.

Figure 6. Variation of entrainment fraction against pipe diameters; comparison between CO2, R11, R12, R22, and R134a.
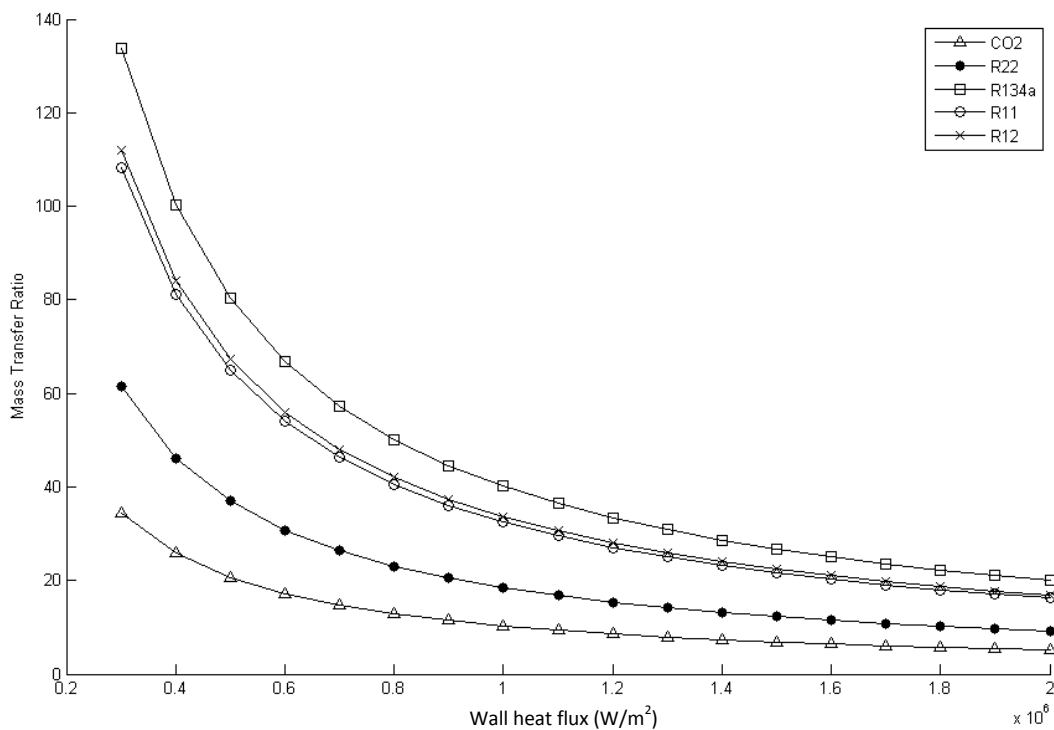

Figure 7. Variation of mass transfer ratio against wall heat flux; comparison between CO2, R11, R12, R22, and R134a.

shown in Figure 7. It can be found from the figure that mass transfer ratio, representing the contribution of entrainment relative to evaporation, takes values that can be hardly ignored. These values emphasize the necessity of considering the effect of entrainment contribution in heat and mass transfer simulation of annular two-phase

flows. Results show that Carbon dioxide has the least mass transfer ratio among the widely-used refrigerants.

Conclusion

R11, R12, R22, R134a as the four widely-used refrigerants are applied in the present study to be compared with carbon dioxide from the entraining treatment point of view. As mentioned in the literatures, carbon dioxide produces more heat transfer and less pressure drop in comparison with conventional refrigerants. Results of the present study have shown that in comparison with commonly used refrigerants, carbon dioxide has much lower values of entrainment in similar conditions. Lower values of entrainment result in lower probability of dry-out occurrence. This issue along with other previously mentioned advantageous has reintroduced CO_2 as a suitable replacement for customary employed refrigerants.

As was shown previously, entrainment contribution of mass transfer is in similar or at some situations higher order than evaporation contribution. This issue signifies the necessity of considering entrainment in simulations of fluid flow and heat transfer of annular two-phase flows. In this regard, a physical entrainment correlation is of great worth. Most of the available correlations of entrainment are empirical and often derived for a specific fluid of special conditions and cannot be generally applied in other situations. Since in the present study, fundamental physics of the entrainment was the basis of deriving the correlation, the proposed formula, is predicted to be applicable for a wide range of applications as it has good consistency with empirical correlations.

Nomenclature: A, Area (m^2); **c,** wave propagation velocity (m/s); **CF,** correction factor; C_w, dimensionless parameter; **E,** entrainment rate (kg/m^2s); **f,** friction factor; F_D, drag force (N); F_g, gravitational force (N), F_σ, surface tension force (N); **g,** gravitational acceleration (m/s^2), **G,** mass flow velocity (kg/m^2s); h_{fg}, enthalpy of evaporation (kJ/kg); **j,** superficial velocity (m/s); **k,** ($=2\pi/\lambda$) wave number; **K,** curvature; **L,** pipe length; N_μ, viscosity number; **p,** pressure (N/m^2), **P;** perimeter (m); q'', heat flux (W/m^2); **Re,** Reynolds number; **t,** time (s); t_w, entrainment period (s); **T,** temperature (K); **u,** velocity (m/s); **x,** axial coordinate (m); x^*, axial coordinate of wave disjoint point; **y,** wave equation.

Greek symbols: λ, Wavelength (m); μ, viscosity ($Pa.s$); ρ, density (kg/m^3); σ, surface tension (N/m); τ, shear stress, (N/m^2), ε, wave amplitude (m); δ, liquid film thickness (m); $\forall$, liquid volume removed from each wave crest (m^3).

Subscripts; co, Vapor core; **en,** entrainment; **ev,** evaporation; **g,** gas; **I,** interface; **I,** imaginary part; **l,** liquid; **R,** real part; **w,** wave.

REFERENCES

Baniamerian Z, Aghanajafi C (2010). Simulation of entrainment mass transfer in annular two-phase flow using the physical concept. J. Mech. 26(3):385-392.

Barbosa JR, Hewitt GF, Konig G, Richardson SM (2002). Liquid entrainment, droplet concentration and pressure gradient at the onset of annular flow in a vertical pipe. Int. J. Multiphas. Flow 28:943-961.

Cheng L, Ribatski G, Wojtan L, Thome JR (2006). New flow boiling heat transfer model and flow pattern map for carbon dioxide evaporating inside horizontal tubes. Int. J. Heat. Mass Tran. 49:4082-4094.

Choi K, Pamitran AS, Oh CY, Oh JT (2007). Boiling heat transfer of R-22, R-134a, and CO_2 in horizontal smooth mini channels. Int. J. Refrig. 30:1336-1346.

Choi K, Pamitran AS, Oh J (2007). Two-phase flow heat transfer of CO_2 vaporization in smooth horizontal mini channels. Int. J. Refrig. 30:767-777.

Collier JG, Thome JR (1996). Convective Boiling and Condensation. Oxford University Press, New York.

Currie IG (1981). Fundamental Mechanics of Fluid. McGraw-Hill, New York.

Hewitt GF, Hall-Taylor NS (1970). Annular Two-Phase Flow. Pergamon Press, Oxford.

Hewitt GF, Whalley PB (1978). The correlation of liquid entrained fraction and entrainment rate in annular two-phase flow. UKAEA Report AERE-9187.

Holowach MJ, Hochreiter FB (2002). A model for droplet entrainment in heated annular flow. Int. J. Heat Fluid Flow 23:807-822.

Kataoka I, Ishii M, Nakayama A (2000). Entrainment and deposition rates of droplets in annular two-phase flow. Int. J. Heat. Mass. Transf. 43:1573-1589.

Oh HK, Ku HG, Roh GS, Son CH, Park SJ (2008). Flow boiling heat transfer characteristics of carbon dioxide in a horizontal tube. App. Therm. Eng. 28:1022-1030.

Okawa T, Kotani A, Kataoka I, Naito M (2003). Prediction of critical heat flux in annular flow using a film flow model. J. Nucl. Sci. Technol. 40:388-396.

Pan L, Hanratty TJ (2002). Correlation of entrainment for annular flow in vertical pipes. Int. J. Multiphas. Flow. 28:363-384.

Sawant P, Ishii M, Mori M (2008). Droplet entrainment correlation in vertical upward co-current annular two-phase flow. J. Nucl. Eng. Des. 238:1342-1352.

Schadel SA, Leman GW, Binder JL, Hanratty TJ (1990). Rates of atomization and deposition in vertical annular flow. Int. J. Multiphas. Flow 16:363-374.

Steinke ME, Kandlikar SG (2004). Single phase heat transfer enhancement techniques in micro channel and mini channel flows. Proceedings of 1st International Microchannels. Minichannels. Conf., New York, USA 126:518-526.

Thomas DA (2002). Modern Geometry. Cole Publishing Co, California.

Thome JR, Ribatski G (2005). State-of-the-art review of flow boiling and two-phase flow of CO_2 in macro- and micro-channels. Int. J. Refrig. 28:1149-1168.

Woodmansee D, Hanratty T (1969). Mechanism for the removal of droplets from a liquid surface by a parallel air flow. J. Chem. Eng. Sci. 24:299-307.

Yun Y, Kim Y, Kim MS (2005). Flow boiling heat transfer of carbon dioxide in horizontal mini tubes. Int. J. Heat Fluid Flow 26:801-809.

Zhao X, Bansal PK (2007). Flow boiling heat transfer characteristics of CO_2 at low temperatures. Int. J. Refrig. 30:937-945.